MASS LOSS CHARACTERISTICS OF DUST FORMING LONG-PERIOD VARIABLE STARS

Jan Martin Winters[1,2,3] & Thibaut Le Bertre[1]

[1] *UMR 8540, Observatoire de Paris, 61 av. de l'Observatoire, F-75014 Paris, France*

[2] *MPI für Radioastronomie, Auf dem Hügel 69, D-53121 Bonn, Germany*

[3] *TU Berlin, Institut für Astronomie und Astrophysik, PN 8-1, Hardenbergstr. 36, D-10623 Berlin, Germany*

winters@mesioc.obspm.fr

Abstract We present results obtained from a grid of model calculations for dust forming circumstellar shells around carbon-rich long-period variable stars. These models consistently treat the time-dependent hydrodynamics, chemistry, dust formation and the radiative transfer problem. We show that variations of the mass loss rates observed on different time scales are well reproduced by our models.

1. INTRODUCTION

In order to investigate the mass loss mechanism of dust forming long-period variable stars (LPVs), we built a grid of $\sim$ 150 carbon-rich hydrodynamic models covering a wide range of physical situations. This grid allows to characterize the effects of the model parameters, i.e. the stellar mass, luminosity, and temperature, the period and amplitude of the pulsation, and the C/O element abundance ratio, on the behavior of AGB winds and on the mass loss rates. A detailed analysis of these calculations is given in Winters et al. (2000a). Here we focus on the general results concerning the outflow characteristics in terms of the wind momentum and on the temporal variation of the mass loss rate on different time scales. To represent the global results of the time-dependent model calculations in a compact way, we introduce a time averaged, dimensionless radiative acceleration $\langle\alpha\rangle_t$, determined in the sub-sonic region of the outflow where dust is condensing. α is the ratio between the radiative acceleration $a^{\rm rad}$ and the gravitational deceleration $a^{\rm grav}$:

$$\alpha \equiv \frac{a^{\rm rad}}{a^{\rm grav}} = \frac{\frac{4\pi}{c}\chi_H H}{\rho G \frac{M_r}{r^2}} = \frac{4\pi\chi_H r^2 H}{c\rho G M_r} = \frac{1}{4\pi c G}\frac{L_*}{M_r}\frac{\chi_H}{\rho} \tag{1.1}$$

(c: speed of light, G: gravitation constant, L_*: stellar luminosity, M_r: mass contained in a sphere of radius r, χ_H: flux-mean extinction coefficient, ρ: mass density, H: Eddington-flux).

2. DEPENDENCE OF THE MODELS ON THE RADIATIVE ACCELERATION

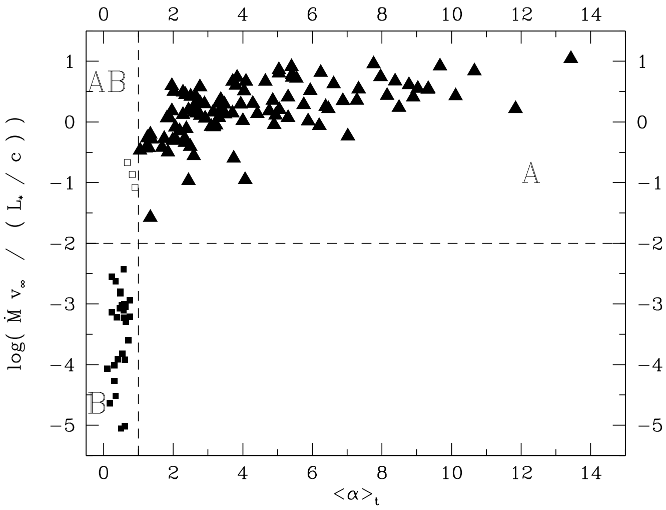

Figure 1 Momentum ratio $\beta = \dot{M} v_\infty/(L_*/c)$ vs. time averaged radiative acceleration $\langle\alpha\rangle_t$

Depending on the value of $\langle\alpha\rangle_t$ we find two regimes for the stellar outflows (see Fig. 1). The first one (regime A, $\langle\alpha\rangle_t > 1$) is characterized by stable winds with a layered structure of the circumstellar dust shell, outflow velocities in the range of $5-40\,{\rm km\,s^{-1}}$, and a large rate of mass loss, $\dot{M} \geq 3\,10^{-7} M_\odot {\rm yr}^{-1}$. For these outflows we find good correlations between near-infrared colors and mass loss rates (see Winters et al. 2000a). In the second regime (B, $\langle\alpha\rangle_t < 1$), the winds are slow, they carry a low mass loss rate ($\dot{M} < 3\,10^{-7} M_\odot {\rm yr}^{-1}$), and they do not present a layered structure. The outflows displaying this second behavior come, e.g., from models with low stellar luminosity, high temperature, or short period. For them there is no correlation between colors and mass loss rates. We have explored the influence of the different parameters (stellar mass, luminosity, temperature, C/O-ratio, pulsation period and -amplitude) on the behavior of the winds. We find that, all other parameters being kept identical, there is a narrow range of values for each parameter within which the models abruptly change from regime B to A, and that once a model is stabilized in the A mode the changes in the values of each parameter have only a smooth effect on the wind characteristics.

In Fig. 1 we represent the global model results in a diagram displaying the ratio β of the momentum carried by the wind ($\dot{M}v_\infty$) to the momentum contained in the radiation field (L_*/c) versus the radiative acceleration $\langle\alpha\rangle_t$. From analytical considerations (e.g., Gail & Sedlmayr 1987) one finds, that there exists a minimum mass loss rate for dust driven winds of the order of $10^{-7}M_\odot\mathrm{yr}^{-1}$, a value which is well reproduced by consistent numerical calculations for stationary dust-driven winds (Dominik et al. 1990) and also by the time-dependent models presented here. In Winters et al. (2000a) the behavior of the mass loss rate $\dot{M}$ and of the outflow velocity v_∞ are discussed separately in terms of the radiative acceleration $\langle\alpha\rangle_t$. It turns out that those models for which the wind is not dominated by radiation pressure (i.e. $\langle\alpha\rangle_t < 1$) always produce low outflow velocities ($v_\infty < 5\,\mathrm{km\,s^{-1}}$). By plotting β on the ordinate in Fig. 1, the separation of the wind models into zone A (dust dominated) and zone B (pulsation dominated) is strongly emphasized by the combined effect of the low mass loss rate and the simultaneously low outflow velocity for the B-models. Once $\langle\alpha\rangle_t$ drops below unity, there is a sudden and very pronounced drop in the momentum ratio β.

Additionally to the models in regions A and B, we find 3 models in the present grid with $\langle\alpha\rangle_t < 1$ and $\beta \approx 10^{-1}$ (region AB). These models show rather regular long term variations of the shell structure and therefore also of $\dot{M}$ and of $\langle\alpha\rangle_t$. Since $\langle\alpha\rangle_t$ is determined in the subsonic wind region around $5R_*$ whereas the mass loss rate is calculated simultaneously outside of $30R_*$, there is a phase shift between the values of $\langle\alpha\rangle_t$ and $\dot{M}$. The models found in region AB have just been caught in a state of high $\dot{M}$ and low $\langle\alpha\rangle_t$.

3. TEMPORAL VARIATION OF THE MASS LOSS RATE

The different types of models found in our grid show temporal variations of the mass loss rate (and, accordingly, of the shell structure) on very different time scales. Therefore, the terms 'mass loss rate' $\dot{M}$ and 'outflow velocity' v_∞ used here refer to temporal averages (usually over 20 pulsation periods) of the respective quantities, defined here as radial

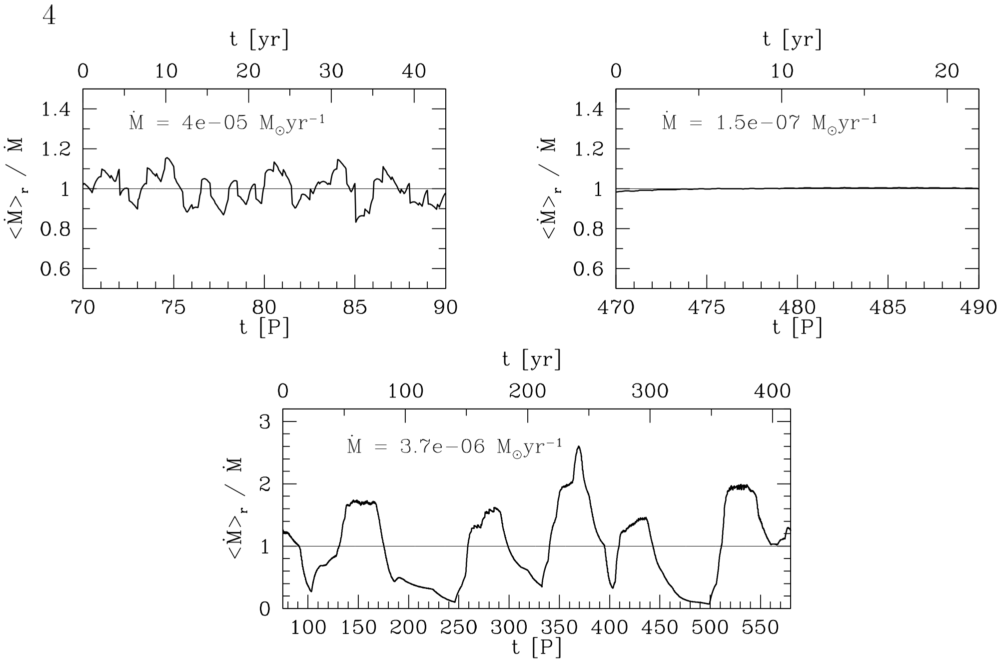

Figure 2 Temporal variation of the mass loss rate of an A-model (upper left), a B-model (upper right) and an AB-model (lower diagram)

mean values in a shell region where dust formation and wind acceleration are complete (in practice, the radial mean values are taken over the shell volume between $30\,\mathrm{R}_*$ and $60\,\mathrm{R}_*$). The temporal variation of the radially averaged mass loss rate, $\langle \dot{M} \rangle_r$, is shown in Fig. 2 for the three different types of models. The A-type models typically show variations of the mass loss rate by about 20% on a time scale of a few pulsation periods (an effect of the *multiperiodicity* discussed by Fleischer et al. 1995). On the contrary, the B-models develop outflow structures which resemble very much those of stationary winds and, therefore, do not display relevant temporal variations of, e.g., the mass loss rate. Finally, the AB models produce rather large variations of the mass loss rate on a typical time scale of the order of 100 yr (note the different scaling in the lower diagram of Fig. 2!). In the three models presently identified as being of the AB type, the outflow velocities are relatively low, $v_\infty \approx 5\,\mathrm{km\,s^{-1}}$ and virtually constant in time.

Apart from the mass loss variations described here, recent evolutionary calculations (Schröder et al. 1999) revealed, for a very limited range of initial stellar masses, a high mass loss rate episode which is connected to a thermal pulse. When the hydrogen-burning shell resumes its energy production after the He shell flash, the star is driven into the A-regime for a time interval of about 1000 yr.

4. EVIDENCE FOR MASS LOSS VARIATIONS FROM OBSERVATIONS

Recent observations indicate the occurrence of variations of the mass loss rates on rather different time scales. For the prominent tip-AGB carbon star IRC +10216, e.g., one finds present-day temporal variations of the shell structure on a time scale of about 10 yr (e.g., Sada 1993, Osterbart et al. 2000, Tuthill et al. 2000, Winters et al. 2000b), resembling the typical *multiperiodicity* time scale found in our A-type models. Imaging of the dust shell around IRC +10216 in scattered galactic light revealed an additional variation of the mass loss rate on a ≈ 100 yr time scale leading to the formation of the so-called multiple layers (Mauron & Huggins 1999, 2000). Also for IRC +10216 one finds from different observational methods (CO rotational line profiles and mapping, CO ro-vibrational line profiles, near-infrared continuum fluxes, 1.3 mm continuum mapping), that the (average) mass loss rate of this object has decreased by a factor of about 5 within the last $\sim$ 5000 yr (e.g., Sahai 1987, Truong-Bach et al. 1991, Keady & Ridgway 1993, Groenewegen et al. 1998). Another type of mass loss variation, which occurs on a ≈ 1000 yr time scale and which most probably is connected to the luminosity variation after a thermal pulse, is evidenced by the presence of thin detached shells around some AGB stars (Olofsson et al. 1996). This kind of mass loss variations explains that, in fact, different observational methods to derive mass loss rates may give very different results. For instance, using CO rotational line data Loup et al. (1993) find $\dot{M} \sim 10^{-5}\,\mathrm{M}_\odot\,\mathrm{yr}^{-1}$ for R Scl, whereas Le Bertre (1997), using IR continuum data, finds $\dot{M} \sim 10^{-7}\,\mathrm{M}_\odot\,\mathrm{yr}^{-1}$, a factor of $\sim$ 100 less. The explanation for this discrepancy lies in a drastic reduction of the R Scl mass loss rate about 100 years ago. The situation is even more complex if one considers the multiple molecular winds recently brought to evidence from composite CO line profiles (Knapp et al. 1998). In these cases, the mass loss rate variations can be uncovered because the properties of the winds, in particular the outflow velocities, are very different. One may suspect that, in other situations where the changes are less radical, such effects would not be detected, but still would affect the determination of $\dot{\mathrm{M}}$. This is particularly true for the CO rotational line method which probes a shell of typically 10^{17} cm in size, formed typically within 3000 years. The IR method is less sensitive to this problem because it is the most internal parts of the circumstellar dust shells ($\sim 10^{15}$ cm in size) which dominate the near-IR continuum emission.

A feature common to all methods for deriving mass loss rates from observations is that an integral of the shell structure along the line of sight is involved (e.g., in terms of column densities, optical depths, or integrated emissivities) and therefore, always some radial averaging is implicitly performed. The radial averaging procedure adopted in the present work for determining the mass loss rate thus very much resembles this aspect of the observational methods.

5. COMPARISON WITH OBSERVATIONS

The variety of different behaviors of the models found in our grid makes it tempting to draw some comparisons to actually observed properties of AGB stars:

A-models: This type of models has been extensively discussed in earlier papers (see Winters et al. (2000a) and references therein) and it has been demonstrated that they reproduce quite well different observed properties of dust forming LPVs. Here we only stress that the effect of multiperiodicity found in these models offers a possible explanation for some of the irregular light curves found, e.g., from the MACHO survey (see Wood et al. (1999) and Wood & Cohen, this volume).

B-models: From the ISOGAL survey, Omont et al. (1999) discovered a population of dust forming sources in the Galactic Bulge with very low mass loss rates, in the range $\dot{M} \approx 10^{-9} M_{\odot} \mathrm{yr}^{-1} \ldots 10^{-7} M_{\odot} \mathrm{yr}^{-1}$. These objects are believed to be in an evolutionary state on the early AGB or near the tip of the Red Giant Branch. The typical luminosity of these sources is relatively low ($L_* \sim 1400 - 3200 L_{\odot}$). The low mass loss rates that we find for the B-type models, which emerge, e.g. for low luminosities, could provide a paradigm for the mass losing low luminosity giants in the Galactic Bulge.

Young (1995) performed a volume limited (d $\leq$ 500 pc) survey of Miras. For most sources which have been detected, the CO lines can be fitted with a one–component wind. Several sources have expansion velocities ≤ 5 km s^{-1}, and one, T Ari, has a $\mathrm{v_{exp}} = 2.7$ km s^{-1}, typical of our B models. Furthermore, Kerschbaum et al. (1996) measured $\mathrm{v_{exp}} = 1.9$ km s^{-1} for the Semiregular variable L^2 Pup, a value again typical of the B-models. In a survey of 45 AGB stars observed in CO with good spectral resolution and good signal-to-noise ratio, Knapp et al. (1998) found in 9 cases evidence for the presence of 2 winds with different expansion velocities. In general, the slow wind has an expansion velocity smaller than 5 km s^{-1} and a mass loss rate smaller than $5\,10^{-7}$ M$_{\odot}$ yr^{-1}, and the opposite for the fast wind. It is tempting to assign the slow wind to the B-type and the fast wind to the A-type models. The presence of winds with very different properties, simultaneously around the same star, can be understood in the framework of our model where a slight change in the stellar parameters may induce a switch from the A to the B mode, or vice versa.

AB-models: One might speculate that the long-term variations of the mass loss rate resulting from the AB-type models could lead to a layered density structure in the extended circumstellar shell which resembles the characteristics of the multiple layers recently found in some carbon-rich proto-planetary nebulae (e.g., Sahai et al. (1998) and Sahai, this volume) but also in the shell of IRC +10216 (Mauron & Huggins 1999, 2000). Although the outflow velocities of our present AB-models are almost constant in time as would be required for such an interpretation, in the present 3 models it is only about 5 $\mathrm{km\,s^{-1}}$, thus a factor of 3 lower than the outflow velocity measured, e.g., for IRC +10216.

Transition from region A to B: As mentioned in the previous sections, a slight change in the stellar parameters (e.g., the stellar luminosity, or the temperature, or a combination of both) may induce a switch of the model from the A-type to the B-type and vice versa. It is exactly this effect, which leads to the abrupt onset and switch-off of the short ($\approx 1000\,\mathrm{yr}$) high mass loss rate episode in our evolution calculations for low initial-mass stars (Schröder et al. 1999). In this case the switch is mainly induced by the luminosity variation following a thermal pulse. This behavior might provide a mechanism to explain the formation of detached shells observed, e.g., around R Scl (see previous Sect.) or around TT Cyg (Olofsson et al. 2000). It is worth stressing that in the context of an excursion in the HR diagram, our models imply that the star is again in the B-mode, after the shell has been expelled. Therefore, we would expect a low present-day mass loss rate ($\dot{M} < 3\,10^{-7} M_\odot \mathrm{yr}^{-1}$) of the central star, carried by a low outflow velocity wind ($v_\infty < 5\,\mathrm{km\,s^{-1}}$). In Table 1 the values observed for 3 of these objects are summarized; they are in perfect agreement with this model prediction.

Table 1 Properties of 3 detached-shell objects

Object	$\dot{M}_{\mathrm{present}}$ $[M_\odot \mathrm{yr}^{-1}]$	Ref.	$v_{\infty,\mathrm{present}}$ $[\mathrm{km\,s^{-1}}]$	Ref.
R Scl	$\sim 10^{-7}$	(1)	?	-
TT Cyg	$3\,10^{-8}$	(2)	3.8	(2)
S Sct	?	-	4.8	(3)

References: (1) Le Bertre (1997), (2) Olofsson et al. (2000), (3) Olofsson et al. (1996)

Acknowledgments

The calculations were performed on the Cray parallel and vector computers of the Konrad-Zuse-Zentrum für Informationstechnik Berlin. Subsequent data analysis has been performed on the WAP–cluster of the physics department of the TU–Berlin. This work has been supported by the BMBF (grant 05 3BT13A 6) and by the PROCOPE program under grants D/9822849 (DAAD) and F/99001 (MAE).

References

Dominik C., Gail H.-P., Sedlmayr E., Winters J.M., 1990, *A&A* 240, 365
Fleischer A.J., Gauger A., Sedlmayr E., 1995, *A&A* 297, 543
Gail H.-P., Sedlmayr E., 1987, *A&A* 177, 186
Groenewegen M.A.T., van der Veen W.E.C.J., Matthews H.E., 1998, *A&A* 338, 491
Keady J.J., Ridgway S.T., 1993, *ApJ* 406, 199
Kerschbaum F., Olofsson H., Hron J., 1996, *A&A* 311, 273
Knapp G., Young K., Lee E., Jorissen A., 1998, *ApJS* 117, 209
Le Bertre T., 1997, *A&A* 324, 1059
Loup C., Forveille T., Omont A., Paul J.F., 1993, *A&AS* 99, 291
Mauron N., Huggins P.J., 1999, *A&A* 349, 203
Mauron N., Huggins P.J., 2000, *A&A* 359, 707
Olofsson H., Bergman P., Eriksson K., Gustafsson B., 1996, *A&A* 311, 587
Olofsson H., Bergman P., Lucas R., et al., 2000, *A&A* 353, 583
Omont A., Ganesh S., Alard C., et al., 1999, *A&A* 348, 755
Osterbart R., Balega Y.Y., Blöcker T., Men'shchikov A.B., Weigelt G., 2000, *A&A* 357, 169
Sada P.A.V., 1993, *Temporal variations in the circumstellar shell IRC +10216*, PhD thesis, New Mexico State University, Las Cruces, USA
Sahai R., 1987, *ApJ* 318, 809
Sahai R., Trauger J.T., Watson K.R., et al., 1998, *ApJ* 493, 301
Schröder K.-P., Winters J.M., Sedlmayr E., 1999, *A&A* 349, 898
Truong-Bach, Morris D., Nguyen-Q-Rieu, 1991, *A&A* 249, 435
Tuthill P., Monnier J., Danchi W., Lopez B., 2000, *ApJ*, in press
Winters J.M., Le Bertre T., Jeong K.S., Helling Ch., Sedlmayr E., 2000a, *A&A* 361, 641
Winters J.M., Keady J.J., Gauger A., Sada P.V., 2000b, *A&A* 359, 651
Wood P.R., Alcock C., Allsman R.A., et al., 1999, In Le Bertre T., Lèbre A., Waelkens C., editors, *IAU Symp. 191: AGB stars*, p. 151
Young K., 1995, *ApJ* 445, 872